Journal of Solid State Chemistry **146,** 1–5 (1999)
Article ID jssc.1999.8218, available online at http://www.idealibrary.com on IDEAL®

Syntheses and Magnetic Properties of $La_{1-x}Sr_xMnO_y$ ($0.5 \leq x \leq 1.0$) Perovskite

K. Kikuchi, H. Chiba, M. Kikuchi, and Y. Syono

Institute for Materials Research, Tohoku University, Katahira, Aoba-ku, Sendai 980-8577, Japan

Received September 21, 1998; in revised form February 9, 1999; accepted February 10, 1999

$La_{1-x}Sr_xMnO_y$ with $0.0 \leq x \leq 0.6$, which reveals very interesting physical properties such as ferromagnetism and metallic resistivity, can easily be synthesized by the conventional solid state reaction. In the case of the composition of $x > 0.6$, they cannot be synthesized by the normal synthesis but by the two-stage solid state reaction, which at first makes the oxygen-deficient state at high temperature and then inserts oxygen by O_2 annealing at low temperature. Nevertheless all of obtained compound is single phase cubic perovskite structure, ferromagnetism and metallic property observed in the composition range $0.175 \leq x \leq 0.6$ are not revealed, cause of drastic change between $0.50 < x < 0.60$.

1. INTRODUCTION

Perovskite manganites of $R_{1-x}A_xMnO_3$ (R = rare earth metal, A = alkaline earth metal) (1, 2) are well known for their interesting physical properties of concurrent ferromagnetism and metallic conductivity in the intermediate composition. Recent reinvestigation of these compounds presented us with an additional interesting phenomenon of an extraordinarily large magnetoresistance effect around T_C (3–5). The crystal structure and various physical properties of $La_{1-x}Sr_xMnO_3$, a representative example of these perovskite manganites, have long been studied, and the ferromagnetism of hole-doped specimens was explained by the so-called double exchange interaction between Mn^{3+} and Mn^{4+} ions (6–10). In this system, hole-doping by the replacement of La with Sr in the parent $LaMnO_3$ results in ferromagnetism for $x > 0.1$ (11, 12).

However, this system can be synthesized only for $0 \leq x \leq 0.6$ as a single phase solid solution by the conventional solid state reaction (hereafter SSR), and the specimens with nominal composition of $0.6 < x < 1.0$ are a two-phase mixture of 4H hexagonal $SrMnO_3$ and cubic $LaSrMnO_3$ with x around 0.6. The crystal structure and the electronic phase diagram were already well investigated (11–14), but little is known about the specimens with $x > 0.6$. In spite of many efforts, synthesis of compounds with $0.6 < x < 1.0$ by SSR was not successful. Recently we succeeded in synthesizing single phase polycrystalline samples in the composition range $0.6 \leq x \leq 1.0$ by using a newly adopted method, two-stage solid state reaction (hereafter, 2-stage SSR). In the course of our study, the physical property of $x = 0.6$ was found to be so different from that of $x = 0.5$ that we investigated for $0.5 \leq x \leq 0.6$ in detail. Here we report the investigation of the crystal structures and magnetic and electrical properties of $La_{1-x}Sr_xMnO_y$ for $0.5 \leq x \leq 1.0$.

2. EXPERIMENTAL

The syntheses of polycrystalline samples of $La_{1-x}Sr_xMnO_3$ with $x = 0.6$, 0.7, 0.8, 0.9, and 1.0 were carried out by using the two-stage SSR according to previous works (15, 16). Starting materials were La_2O_3, Mn_2O_3, and $SrCO_3$. La_2O_3 and Mn_2O_3 were calcined in air at 700°C for 3 hours and several days, respectively, to remove absorbed water of La_2O_3 and to keep proper valence of Mn_2O_3. Mixtures of $(1-x)/2La_2O_3 + 1/2Mn_2O_3 + xSrCO_3$ were stirred with acetone for 15 minutes in a ball mill and were dried.

At first, we attempted reexamination of previous synthesis of $SrMnO_3$ with the perovskite structure. 4H hexagonal $SrMnO_3$ was obtained by using a conventional solid state reaction technique (17). Then, it was converted to an oxygen deficient perovskite structure (18, 19) by heating at 1400°C under Ar (first stage). Finally, it was annealed at 350°C in air for 1 week to obtain the oxygen-filled $SrMnO_3$ with the perovskite structure (second stage). For the composition of $0.6 \leq x \leq 0.9$, the samples were prefired at 1000°C and finally fired at 1400°C under Ar and then annealed at 350–450°C in air for several days. To ensure oxygen content, the specimens were treated by the HIP technique under high oxygen pressure. To explain the drastic change of physical property from $x = 0.5$ to $x = 0.6$, we also investigated these specimens in detail. The specimens of $La_{1-x}Sr_xMnO_3$ for $x = 0.50$–0.60 at 0.02 intervals were

0022-4596/99 $30.00

synthesized by both SSR and two-stage SSR. In SSR, the samples were prefired at 1000°C and finally fired at 1350°C under air.

The prepared specimens were examined by X-ray powder diffraction (XRD) using monochromated Cu$K\alpha$ radiation. The unit cell dimensions were determined from the observed *d*-spacings by least squares method. The analysis of the oxygen content of the final products was carried out by using an iodine titration method with AUT301. The thermogravimetry (TGA) measurement was carried out by using TGD-7000. TEM work was carried out by using JEM-2000EX.

Temperature dependence of magnetic susceptibility and resistivity for these samples were examined by using a superconducting quantum interference device magnetometer (Quantum Design) and a four-probe method, respectively.

3. RESULTS AND DISCUSSION

3.1. X-Ray Analysis and Thermogravimetry

Figure 1 shows the temperature change of oxygen content, y, of $La_{1-x}Sr_xMnO_y$ measured by TGA. The starting sample was prepared as an oxygen-deficient perovskite. TGA measurements were carried out in oxygen atmosphere at a heating rate of 200°C per hour. The oxygen absorption of each specimen started from about 200°C and finished at about 300°C. The oxygen content of the oxygen-filled state was determined by the iodine titration method, and that of the oxygen-deficient state was calculated from the results of thermogravimetry. Although all the oxygen numbers of the oxygen-filled state were about 3, that of the oxygen-deficient state varied from 2.56 to 2.87 with decreasing x. This shows that it becomes difficult to make oxygen-deficient perovskite with increasing La content.

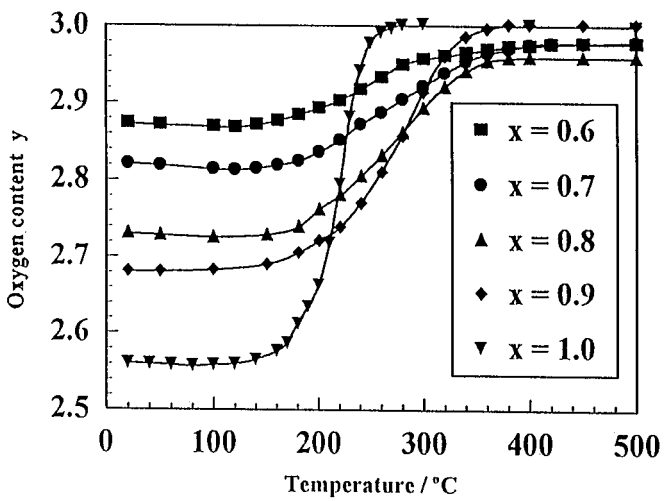

FIG. 1. The absorption of oxygen with increasing temperature revealed by TGA measurement.

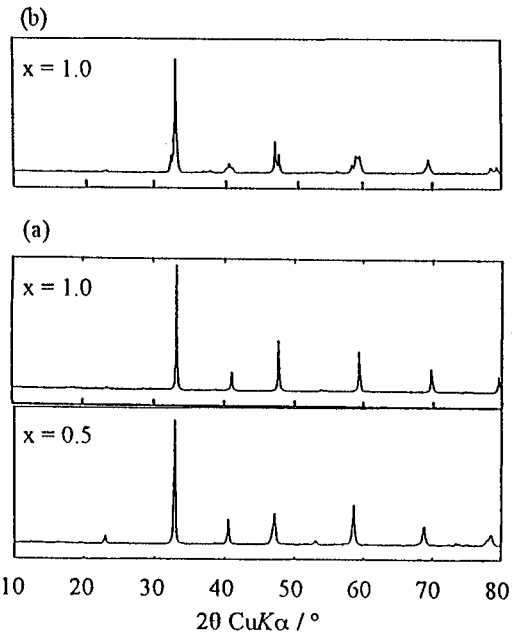

FIG. 2. XRD patterns at room temperature for oxygen-filled states with $x = 0.5$ and 1.0 (a), and oxygen-deficient state with $x = 1.0$ (b). Oxygen-filled states were all in a cubic system, and oxygen-deficient states were also cubic except for $x = 1.0$, where orthorhombic distortion was observed owing to ordering of 0.5 oxygen vacancy.

XRD patterns of the oxygen-filled state specimens with $x = 0.5$ and 1.0 and oxygen-deficient state specimen with $x = 1.0$ are shown in Fig. 2. The reflection peaks were indexed on the basis of the cubic perovskite lattice except for $x = 0.6$. There was small splitting of high-angle diffraction peaks of $x = 0.6$ and the tetragonal unit cell was adopted. It is known that when the oxygen-deficiency is 0.5 (1/6 of whole oxygen content), the crystal structure of $SrMnO_{2.5}$ changes from a cubic perovskite to an orthorhombic form due to the ordering of oxygen vacancies. Other specimens did not show ordering and remained in the cubic system. This seems to be cause by the decrease in the amount of oxygen deficiency. The amount of oxygen deficiency of the samples with $x = 0.6$–0.9 was too small for oxygen vacancy ordering. The superstructure due to the oxygen vacancy ordering was not observed in the electron diffraction pattern of all specimens. The specimens with $x = 0.50$, 0.52, 0.54, and 0.56 were able to be synthesized as single phase by SSR, but $x = 0.58$ and $x = 0.60$ were obtained as a mixed phase of cubic and hexagonal $SrMnO_3$ phases. On the other and, all specimens of this region were able to be synthesized as a single phase by two-stage SSR (Table 2). All of them were with the cubic system, but become slightly distorted to tetragonal after O_2 annealing.

TABLE 1
Summary of Lattice Parameter a of $La_{1-x}Sr_xMnO_y$

Nominal composition (x)	a/Å of $La_{1-x}Sr_xMnO_y$		
	Before annealing (oxygen deficient)	After annealing (oxygen filled)	After HIP (1500 atm)
0.6	3.871[a]	3.847[a]	3.852[a]
0.7	3.867	3.838	3.835
0.8	3.856	3.823	3.825
0.9	3.849	3.818	3.816
1.0	—[b]	3.805	3.811

[a] Calculated as a pseudo-cubic system.
[b] This sample is not cubic but an orthorhombic system with $a = 5.496$ Å, $b = 15.238$ Å, $c = 5.415$ Å.

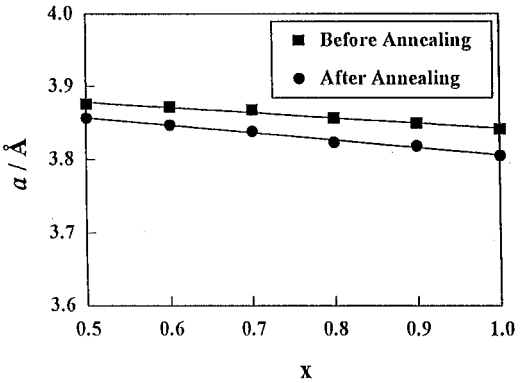

FIG. 3. Composition dependence of cell parameter a in the system $La_{1-x}Sr_xMnO_y$.

3.2. Magnetic and Electrical Properties

The unit cell parameters are summarized in Table 1 and plotted against Sr content, x, in Fig. 3. The lattice parameters decreased with increasing x. When the oxygen-deficient sample was annealed, the lattice parameter was reduced owing to the increase in Mn^{4+} content because of a smaller Mn^{4+} than Mn^{3+}.

The SQUID measurements with a magnetic field of 1 T were carried out for all synthesized specimens. The temperature dependence of magnetization per Mn atom for $x = 0.6$–1.0 is shown in Fig. 4. In the case of $SrMnO_3$, a small anomaly at 250 K as seen in Fig. 4 is consistent with T_N determined by neutron diffraction in a previous work (15). A large increase of magnetization at low temperature seems to be due to magnetic impurities in the sample, for example, Mn_3O_4 with $T_C = 40$ K. Although ferromagnetism was observed for $x \leq 0.6$ in previous works (11–13), the present specimens of $0.6 \leq x \leq 1.0$ did not reveal any ferromagnetic behavior.

TABLE 2
Summary of Oxygen Contents of $La_{1-x}Sr_xMnO_y$
($0.50 \leq x \leq 0.60$)

Nominal composition (x)	SSR (y)	Two-stage SSR (y)	
		O_2 deficient	O_2 filled
0.50	2.99	—[b]	3.01
0.52	2.99	2.89	3.01
0.54	3.00	2.80	3.01
0.56	3.01	2.76	3.02
0.58	2.99[a]	2.82	3.01
0.60	2.99[a]	—[b]	3.01

[a] These samples are not single phase.
[b] These samples' data were not measured.

The electrical resistivity (r) measurements were carried out down to 20 K. Resistivities of all the specimens showed a semiconducting temperature dependence and became too high to be measured at low temperatures. The temperature dependence of electrical resistivity is shown in Fig. 5. A small anomaly observed around 25 K for samples of $0.6 \leq x \leq 0.9$ seems to be consistent with that of magnetization, but the origin of the transitions is still not clear. The metallic behavior observed for $0.175 \leq x \leq 0.6$ (11–13) was not observed in $0.6 \leq x \leq 1.0$.

To explain the drastic change of magnetic property from $x = 0.5$ to $x = 0.6$, we investigated between $x = 0.5$ and $x = 0.6$ in detail. Magnetic and electric properties were measured by the same way of $x = 0.6$–1.0. Ferromagnetic $La_{1-x}Sr_xMnO_y$ could be synthesized by conventional SSR method for only $x \leq 0.56$. On the contrary, cubic single phase could be synthesized for all of $0.50 \leq x \leq 0.60$ by two-stage SSR synthesis, but ferromagnetic behavior in low temperature suddenly disappeared as seen in Fig. 4. Ferromagnetism was observed down to liquid He temperature for $x = 0.50$, but a sudden decrease of magnetization occurred at a critical temperature around 200 K for $x = 0.52$. The critical temperature where magnetization began to decrease increased with increasing x. Suppression of ferromagnetism suggests different magnetic order (probably antiferromagnetic order) below the T_C. The appearance of the antiferromagnetic metal below T_C is considered to be due to the double exchange mechanism only within the c-plane and interplane antiferromagnetic interaction, because the c-axis of the unit cell was elongated by the distortion from cubic to tetragonal. The behavior of the sharp peak seen in $x = 0.6$ cannot be interpreted by the change order observed in the system of $Bi_{1-x}Ca_xMnO_3$ (20), because the super spots due to charge order were not observed by TEM work, and the electric property of the specimen with $x = 0.6$ was still metallic (21).

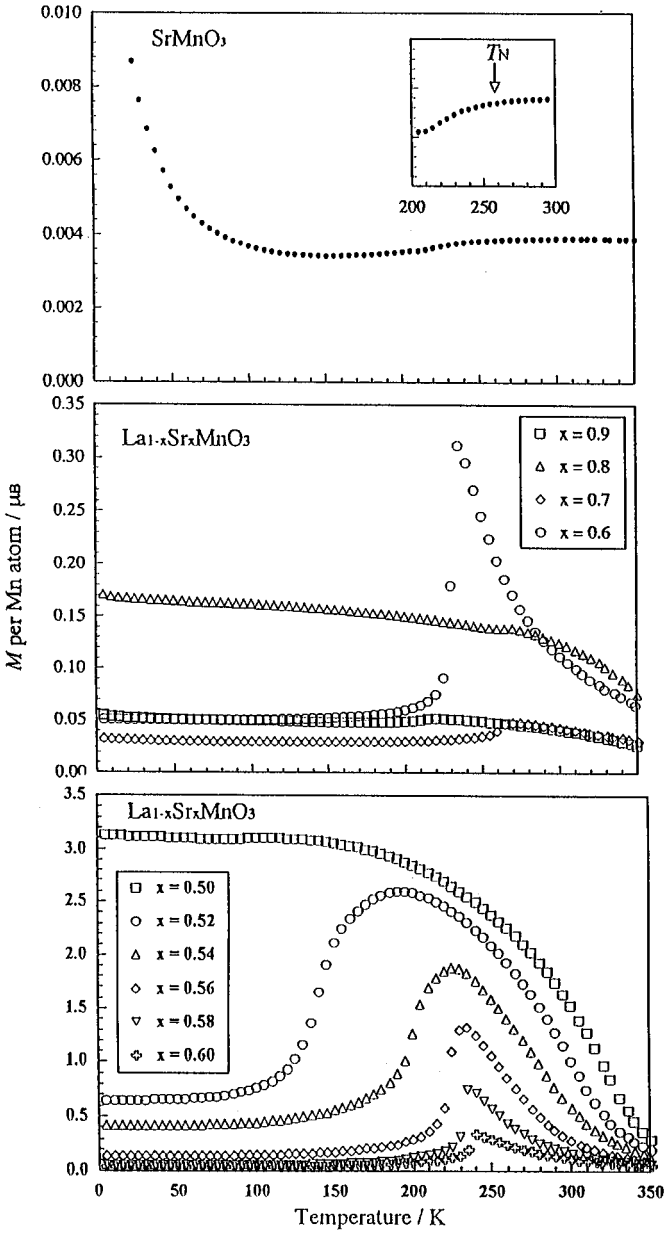

FIG. 4. Temperature dependence of magnetization of $La_{1-x}Sr_xMnO_y$ ($x = 0.5$–1.0) measured at 1 T.

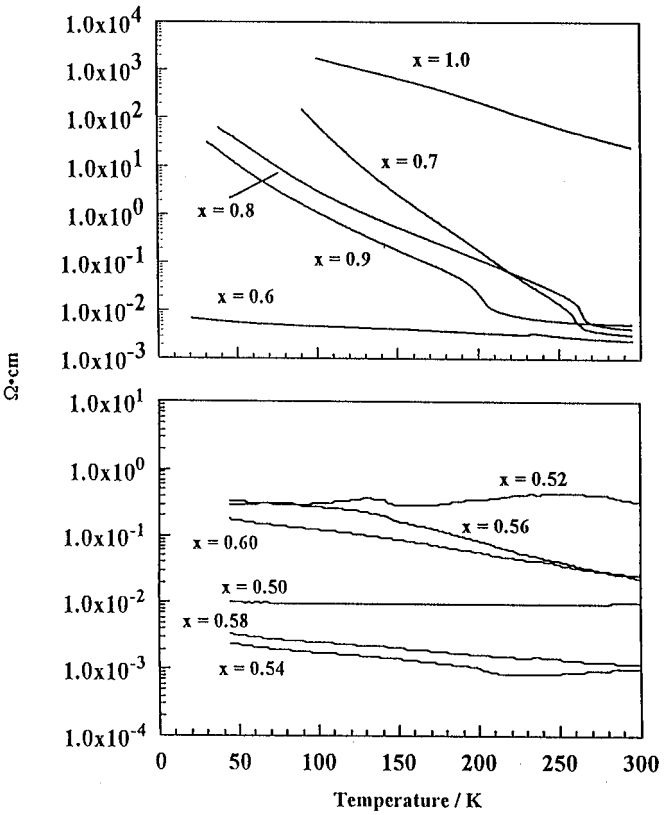

FIG. 5. Resistivity of $La_{1-x}Sr_xMnO_y$ ($x = 0.5$–1.0) versus temperature measured by four-probe method.

4. SUMMARY

Single phase perovskite structure manganites of $La_{1-x}Sr_xMnO_3$ with $0.5 \leq x \leq 1.0$ have been synthesized, and magnetic and electrical properties have been investigated for synthesized specimens. With $0.6 \leq x \leq 1.0$, $La_{1-x}Sr_xMnO_3$ can be synthesized by using two-stage SSR in which an oxygen-deficient state was achieved by calcining at 1400°C under Ar, and then doping O_2 was made by annealing at low temperature under air or O_2. In this region, ferromagnetism and metallic behavior observed in a low Sr doped region are not observed. Ferromagnetic behavior was observed up to $x = 0.50$. Ferromagnetism was found to disappear suddenly around 200 K for $x \geq 0.52$ and completely vanished for $x > 0.6$.

ACKNOWLEDGMENT

We thank H. Tokuno, H. Aoyagi, and S. Hayasaka (IMR, Tohoku Univ.) for their help in technical support. We thank T. Atou, K. Kusaba, and H. Faqir for useful discussions and assistance.

REFERENCES

1. J. B. Goodenough, *Phys. Rev.* **100,** 564 (1955).
2. G. H. Jonker and J. H. Van Santen, *Physica*, **16,** 337 (1950).
3. P. Schiffer, A. P. Ramirez, W. Bao, and S.-W. Cheong, *Phys. Rev. Lett.* **75,** 3336 (1995).
4. S. Jin, T. H. Tiefel, M. McCormack, R.A. Fastnacht, R. Ramesh, and L. H. Chen, *Science* **264,** 413 (1994).
5. R. von Helmolt, J. Wecker, B. Holzapfel, L. Schultz, and Samwer, *Phys. Rev. Lett.* **71,** 2331 (1993).
6. C. Zener, *Phys. Rev.* **82,** 403 (1951).
7. P. W. Anderson and H. Hasegawa, *Phys. Rev.* **100,** 675 (1955).

8. P.-G. de Gennes, *Phys. Rev.* **118,** 141 (1960).
9. C. W. Searle and S. T. Wang, *Can. J. Phys.* **47,** 2703 (1969).
10. K. Kubo and N. Ohata, *J. Phys. Soc. Jpn.* **33,** 21 (1972).
11. J.-S. Zhou, J. B. Goodenough, A. Asamitsu, and Y. Tokura, *Phys. Rev. Lett*. **79,** 3234 (1997).
12. A. Urushibara, Y. Moritomo, T. Arima, A. Asamitsu, G. Kido, and Y. Tokura, *Phys. Rev. B* **51,** 14103 (1995).
13. H. Kawano, R. Kajimoto, M. Kubota, and H. Yoshizawa, *Phys. Rev. B* **53,** R14709 (1996).
14. A. Asamitsu, Y. Morimoto, Y. Tomioka, T. Arima, and Y. Tokura, *Nature* **373,** 407 (1995).
15. T. Takeda, and S. Ohara, *J. Phys. Soc. Jpn.* **37,** 275 (1974).
16. N. Mizutani, A. Kitazawa, N. Okuma, and M. Kato, *J. Chem. Soc. Jpn.* **73,** 1097 (1970); **73,** 1103 (1970).
17. T. Negas, and R. S. Roth, *J. Solid State Chem.* **1,** 409 (1970).
18. E. O. Wollan and W. C. Koehler, *Phys. Rev.* **100,** 545 (1955).
19. A. Reller, J. M. Thomas, D. A. Jafferson, and M. K. Uppal, *Proc. R. Soc. Lond. A* **394,** 223 (1984).
20. H. Chiba, M. Kikuchi, K. Kusaba, Y. Muraoka, and Y. Syono, *Solid State Commun.* **99,** 499 (1996).
21. Y. Moritomo, T. Akimoto, A. Nakamura, K. Ohoyama, and M. Ohashi, *Phys. Rev. B* **58,** 5544 (1998).